Catalysis Science & Technology

PAPER

View Article Online
View Journal | View Issue

Cite this: *Catal. Sci. Technol.*, 2018, **8**, 3539

Electron donor-free photoredox catalysis *via* an electron transfer cascade by cooperative organic photocatalysts†

Lei Wang, Irina Rörich, Charusheela Ramanan, Paul W. M. Blom, Wei Huang, Run Li and Kai A. I. Zhang *

Electron-donating sacrificial reagents are highly important for certain photo-redox reactions. However, the use of excessive amounts of sacrificial reagents, mostly amines, often leads to undesired side products and is especially troublesome for product purification. Herein, we take the light-induced electron transfer cascade process of natural photosystems as a role model and assemble organic photocatalysts into cooperative photocatalyst couples. The cooperative photocatalyst couples could undergo intermolecular electron transfer to facilitate the charge separation process and overcome the need for an extra electron donor. Time-resolved photoluminescence spectroscopy was conducted to precisely characterize the photo-excited dynamics within the cooperative photocatalyst couples. As a model photoredox reaction, the carbon–carbon formation reaction between heteroarenes and malonates, which usually requires electron-donating sacrificial reagents such as amines, was conducted to demonstrate the feasibility of the cooperative photocatalyst couples under visible light irradiation. A significant reaction conversion improvement from trace conversion for a single photocatalyst system to over 90% by cooperative photocatalyst couples was achieved.

Received 25th May 2018,
Accepted 20th June 2018

DOI: 10.1039/c8cy01072b

rsc.li/catalysis

Introduction

Electron-donating sacrificial reagents are of great importance for photocatalytic redox reactions including chemical transformation and water decomposition into hydrogen and oxygen.[1–3] Especially for semiconductor-catalyzed reactions, the catalytic efficiency can be largely improved while the photo-generated holes can be scavenged by the electron-donating reagent molecules and the charge recombination can be reduced.[2] Examples of organic photoredox reactions without the employment of sacrificial reagents were conducted using reactive substrates such as aryl diazonium[4] or trifluoromethanesulfonyl salts,[5] as well as when the solvent molecule could also act as an electron donor.[6] However, for specific photoredox reactions involving less reactive substrates, the use of electron donating reagents is necessary. And the use of usually excessive amounts of donor reagents during the catalytic cycle, mostly amines,[7–10] often leads to undesired oxidized side products and is especially troublesome for product purification.[11] To overcome the above-mentioned challenge and maintain reduced charge recombination within the semiconductor-based photocatalyst, an enhanced photo-generated electron transfer pathway should be developed.

Natural photosystems offer a promising model to overcome the charge recombination issue, where a series of stepwise electron transfer processes are involved to enhance the photogenerated charge separation and transfer process.[12] So far, chemists have designed different photocatalytic systems for enhancing the photocatalytic efficiency. For example, bridged transition metal complexes[13–15] have been reported

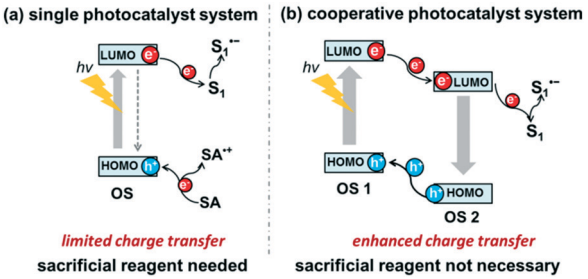

Fig. 1 Difference between (a) a conventional single organic photocatalyst system with direct electron/hole recombination, where a sacrificial reagent is needed, and (b) a cooperative photocatalyst system with enhanced electron/hole separation *via* an electron transfer cascade, where no sacrificial reagent is needed. OS: organic semiconductor; SA: sacrificial electron donor reagent; S: substrate.

Max Planck Institute for Polymer Research, Ackermannweg 10, 55128 Mainz, Germany. E-mail: kai.zhang@mpip-mainz.mpg.de

† Electronic supplementary information (ESI) available: Experiment details and characterization, ^{1}H and ^{13}C NMR spectra, fluorescence quenching experiments and control experiments are described. See DOI: 10.1039/c8cy01072b

to greatly promote the photogenerated charge separation and transfer.

Organic semiconductor (OS)-containing photocatalysts have emerged as a promising alternative to traditional metal-containing photocatalysts due to their highly tunable electronical properties *via* flexible structural design. Recent research activities have demonstrated a vast number of structural design methods of small molecular[8,10,16–20] or macromolecular[21–30] OS systems as efficient photocatalysts for visible light-promoted photoredox reactions. Nevertheless, most developed OS photocatalysts, similar to traditional transition metal complexes,[31–38] are single photocatalytic systems. As illustrated in Fig. 1a, the photocatalytic ability of the OS system originates from the photo-generated electron/hole pair, which can function as the reductive and oxidative species. To maintain the efficient electron transfer from the ground to the exited state of the OS, extra sacrificial agents are usually needed due to direct recombination of the electron/hole pair. To overcome the necessary use of electron-donating sacrificial reagents, the single photocatalyst system is not sufficient; a new concept of catalyst design is needed.

Herein, we aim to take the mechanism of the light-induced electron transfer cascade process of natural photosystems as a role model and assemble organic photocatalysts into cooperative photocatalyst couples. As illustrated in Fig. 1b, the two molecular OS photocatalysts within the cooperative couple consisted of different organic photocatalysts possessing different highest occupied molecular orbital (HOMO) and lowest unoccupied molecular orbital (LUMO) levels. By coupling the OSs, an extra intermolecular electron transfer could occur between the OSs, leading to enhanced photo-generated electron/hole separation under light irradiation and thereby more stable reductive and oxidative species. The intermolecular electron transfer within the OS couple can decay the direct recombination of the electron/hole pair and overcome the mandatory requirement of extra electron donors during the photoredox cycle. As a model reaction, the photocatalytic carbon–carbon formation reaction between electron-rich heteroarenes and malonates, which usually required electron-donating sacrificial reagents,[9,39] was chosen to demonstrate the feasibility and photocatalytic activity of the cooperative photocatalyst couple. No extra sacrificial reagents were needed. The light-induced electron transfer between the OSs within the cooperative photocatalyst couple and the substrates could be revealed by mechanistic studies.

Results and discussion

In this study, three molecular organic semiconductors (OS), in particular, 4,7-di(thiophen-2-yl) benzo[*c*][1,2,5]thiadiazole (Th-BT-Th), 2-butyl-4,7-di(thiophen-2-yl)-2*H*-benzo[*d*][1,2,3]-triazole (Th-BTz-Th), and 4,7-bis(1-butyl-1*H*-1,2,3-triazol-4-yl)benzo[*c*] [1,2,5]thiadiazole (TA-BT-TA) were designed. The structures and energy band positions of the OSs are shown in Scheme 1. The synthetic and characteristic details of the OSs are described in the Experimental section or the ESI.†

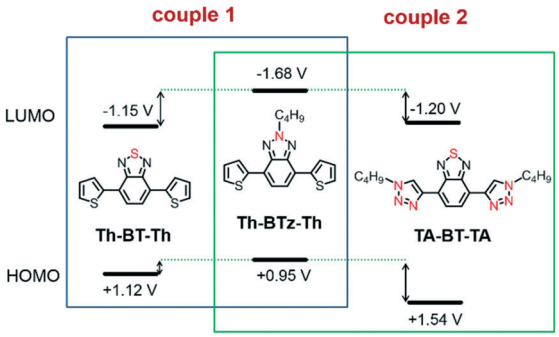

Scheme 1 Structure and HOMO/LUMO levels (*vs.* SCE) of the OS molecules in both designed photocatalyst couples.

The three OSs possessed different HOMO and LUMO band positions, which could be determined *via* cyclic voltammetry (Fig. S1†). As shown in Scheme 1, Th-BTz-Th exhibited a significantly high LUMO level at −1.68 V *vs.* saturated calomel electrode (SCE), followed by TA-BT-TA with −1.20 V *vs.* SCE and Th-BT-Th with −1.15 V *vs.* SCE. In comparison, TA-BT-TA exhibited the lowest HOMO level at +1.54 V *vs.* SCE, followed by Th-BT-Th with +1.12 V *vs.* SCE and Th-BTz-Th with +0.95 V *vs.* SCE. In addition, the excited state redox potentials are calculated to be +1.16 V and −1.01 V *vs.* SCE for Th-BT-Th, +0.62 V and −1.35 V *vs.* SCE for Th-BTz-Th, and +1.14 V and −0.80 V *vs.* SCE for TA-BT-TA, respectively. The data are listed in Table S1 in the ESI† using the calculation described in a previous report.[40] Given the different energy band positions, we assembled the three OSs in two photocatalyst couples for this study, particularly, Th-BTz-Th/Th-BT-Th for cooperative photocatalyst couple 1 and Th-BTz-Th/TA-BT-TA for couple 2.

Steady-state fluorescence quenching experiments showed that by only exciting Th-BT-Th (at 500 nm) or TA-BT-TA (at 450 nm) in both couples, the fluorescence intensity of couple 2 exhibited a larger decrease in PL intensity than that of couple 1, indicating an enhanced electron transfer within couple 2, which was likely caused by the larger distance between the two HOMO levels (Fig. S2†).

To further study the photo-induced charge transfer within the couples, time-resolved photoluminescence (TRPL) spectroscopy was conducted to characterize the photo-excited dynamics within the OS couples. The PL measurements of the pristine materials and a 1 : 1 (mol%) blend were all performed in DMF solution with excitation at 400 nm (Fig. 2c and d). The selected PL decays correspond to the emission maximum for each component OS (Fig. 2c). The fluorescence features of the different component materials overlap with each other. Therefore, the decay associated spectra (DAS) were derived by a global fitting analysis[41] of the TRPL data (Fig. S2†). This allows us to characterize the spectral distribution and lifetime of each emitting species, particularly for the measurements of couple 1 and couple 2. In couple 1 (Fig. S2a†), one can see that DAS 1, centered at 460 nm, matches exactly with the fluorescence spectrum of Th-BTz-Th and decays in 0.6 ns, which is quenched with respect to the pristine donor (2.6 ns). DAS 2, which is centered at 590 nm,

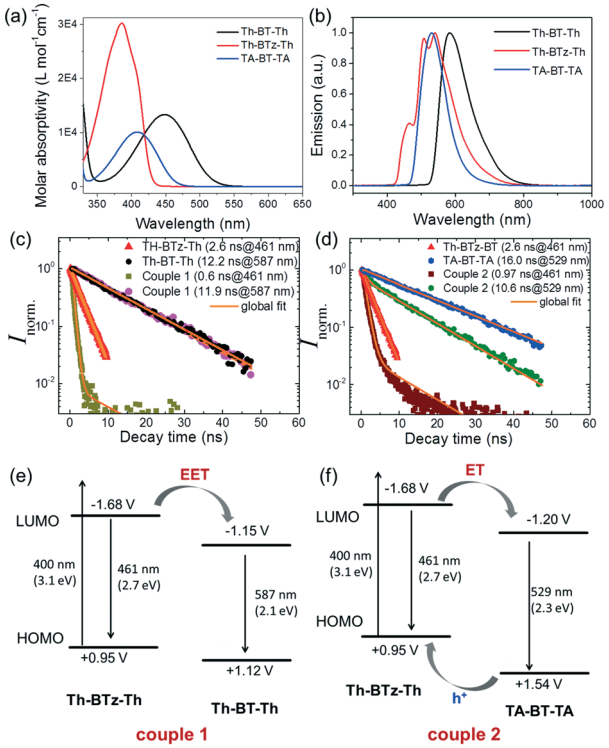

Fig. 2 (a) UV/vis absorption and (b) fluorescence spectra of the three OS molecules. (c) and (d) PL decay times of the pristine materials and the blend of the cooperative couples with exciton lifetimes collected at the fluorescence maximum. (e) and (f) Jablonski diagram illustrates the energy and charge transfer in the photocatalyst couples, respectively. Excitation wavelength: 400 nm. EET: excitation energy transfer; ET: electron transfer.

matches the fluorescence spectrum of Th-BT-Th and decays with the same ~12 ns lifetime as the pristine Th-BT-Th sample, exhibiting no quenching. This indicates that in couple 1 the excitation energy transfer (EET) from Th-BTz-Th to Th-BT-Th likely dominates the excited state dynamics, as illustrated in Fig. 2e. In couple 2 (Fig. S2b†), the DAS 1, centered at 460 nm, originates again from Th-BTz-Th and decays in 0.97 ns, which is quenched with respect to the pristine Th-BTz-Th (2.6 ns). DAS 2, centered at 530 nm, is assigned to the emission of TA-BT-TA and has a decay time of 10.6 ns. Here, the fluorescence of both Th-BTz-Th and TA-BT-TA is quenched with respect to the pristine materials. This indicates an electron transfer from Th-BTz-Th to TA-BT-TA and an enhanced charge transfer within couple 2 (Fig. 2f).

We chose the photocatalytic carbon–carbon formation reaction between electron-rich heteroarenes and malonates as a model reaction.[9,10] Previous studies demonstrated the mandatory use of sacrificial reagents, mostly amines, which ought not to only act as electron donors, but also as electron mediators between the radical intermediate and the photogenerated hole of the photocatalyst (Fig. S4†). We first tested the three designed OSs as single photocatalyst systems without using sacrificial reagents. As expected, by using 3-methylbenzofuran and diethyl bromomalonate in the model reaction, no product was obtained using Th-BT-Th and TA-BT-TA as photocatalysts (entries 1 and 2 in Table 1). Interestingly, using Th-BTz-Th as a photocatalyst led to a slight conversion of 9%. This indicates that a minimal electron transfer could still occur between the photocatalyst and the substrate, which corresponds to the highest LUMO level of Th-BTz-Th among the three OSs and thereby the largest overpotential for the reduction of diethyl bromomalonate.

In contrast, by using both cooperative photocatalyst couples, the product could be obtained in significantly higher conversions, in particular, 43% for couple 1 and 93% for couple 2 (entries 4 and 5). Both the apparent quantum yield (Φ_{AQY}) and catalytic turnover number (TON) for the model reaction (entry 5) using coupling 2 as a photocatalyst were calculated to be 0.04% and 8.7, respectively (ESI†). A kinetic study confirmed the superior catalytic activity of couple 2 compared to couple 1 *via* a fluorescence quenching experiment by the substrates (Fig. S6†). This is in agreement with the photophysical study (Fig. 2), indicating that the enhanced charge transfer between Th-BTz-Th and TA-BT-TA in couple 2 led to a better catalytic efficiency than that of couple 1 containing Th-BTz-Th and Th-BT-Th. The reason could lie on the larger HOMO energy gap (ΔE_{HOMO} = 0.59 V) between Th-BTz-Th and TA-BT-TA than that (ΔE_{HOMO} = 0.17 V) in couple 1 between Th-BTz-Th and Th-BT-Th.[42,43] By using a single wavelength light source (blue LED, 450 nm), where only TA-BT-TA of couple 2 could be excited, the model reaction exhibited a high conversion of 98%. This indicates a hole transfer from TA-BT-TA to Th-BTz-Th, leading to a similar effect of an electron transfer from Th-BTz-Th back to TA-BT-TA, as illustrated in Fig. 2f.

In comparison with the use of Th-BT-Th as a single photocatalyst with the employment of an extra sacrificial electron donor, in particular, triphenylamine from our previous report for the model reaction,[44] where the apparent quantum yield was calculated to be 0.96%, the apparent quantum yield of couple 2 was lower due to the longer reaction time. However, the avoidance of the extra sacrificial electron donor using the molecular photocatalyst couples is still advantageous. It can efficiently prevent the post-purification procedures caused by the addition of usually excess amounts of amine donors.

Screening experiments using different substrates confirmed the feasibility of the OS couple as a photocatalyst (entries 7–9). Other control experiments either without the photocatalyst or without light led to no product formation (entries 12 and 13), indicating the mandatory roles of both components.

To gain more mechanistic insight into the interaction between the photocatalyst and substrate, we conducted further fluorescence quenching experiments. It was shown that the fluorescence of the OSs as single photocatalysts could be only minimally quenched by adding diethyl bromomalonate (Fig. S5†). In contrast, the fluorescence of both photocatalyst couples could be gradually quenched by adding diethyl bromomalonate (Fig. S6†), confirming the possible electron transfer between the photocatalyst couple and the substrate.

To precisely study the actual electron transfer process within the catalytic cycle, we then employed ethyl bromoacetate as a substrate, which possessed a reduction potential

Table 1 Photocatalytic C–C bond formation between diethyl bromomalonate and heteroarenes using different photocatalyst systems[a]

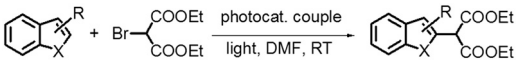

Entry	Catalyst	Substrate	Product	Conv[b] [%]	Yield[c] [%]
1	Th-BT-Th		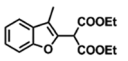	Trace	—
2	TA-BT-TA		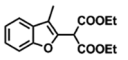	0	—
3	Th-BTz-Th		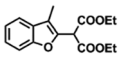	9	—
4	Couple 1		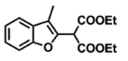	43	39
5	Couple 2		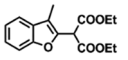	93	87
6[d]	Couple 2		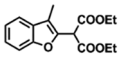	98	85
7[e]	Couple 2		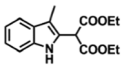	78	75
8[e]	Couple 2		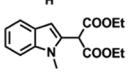	92	85
9[e]	Couple 2	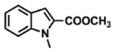	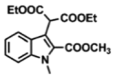	85	80
10[f]	Th-BTz-Th/TA-BT-TA (2 : 1)		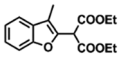	72	60
11[f]	Connected cat.		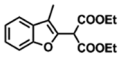	31	22
12[g]	—		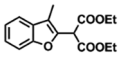	0	—
13[h]	Couple 2		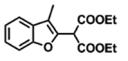	0	—

[a] Reaction conditions: 1 equiv. (0.38 mmol) heteroarene, 2 equiv. diethyl bromomalonate, 0.1 equiv. photocatalyst (for the coupled system, the ratio between the two OSs was 1 : 1) in 2.5 mL DMF, white LED lamp (0.07 Wcm^{-2}), 24 h. [b] Determined by GC-MS. [c] Isolated yield. [d] Blue LED (450 nm, 0.1 Wcm^{-2}). [e] 48h. [f] 0.05 equiv. photocatalyst, 24 h. [g] No catalyst, under light. [h] No light.

of −1.43 V *vs.* SCE (Fig. 3). By using couple 2 as a photocatalyst, it could be determined that only traces of the final product could be obtained (Fig. S11†). This reveals that the photo-generated electron could indeed only transfer from the LUMO of Th-BTz-Th (−1.68 V *vs.* SCE) to the LUMO of TA-BT-TA (−1.20 V *vs.* SCE) in the first step, from which the further electron transfer to the higher reduction level of ethyl bromoacetate was not possible. Additionally, a direct electron transfer from Th-BTz-Th to ethyl bromoacetate could not occur either. In comparison, diethyl bromomalonate ($E_{red.}$ = −1.00 V *vs.* SCE) could be reduced *via* electron transfer originating from the LUMO of TA-BT-TA, leading to the formation of the malonate radical, which further reacts with 3-methylbenzofuran to form the final product in the following step of the catalytic cycle. An additional model reaction using Th-BTz-Th as the single photocatalyst system and triphenylamine as the sacrificial reagent led to the formation of the final product, confirming that a direct electron transfer from Th-BTz-Th to ethyl bromoacetate was only possible in the absence of TA-BT-TA (Fig. S12†). It is also worth noting that further scope reactions with other substrates led to high product yields using couple 2 as a photocatalyst, demonstrating the general feasibility of the cooperative photocatalyst design. It is worth noting that a possible radical chain mechanism as introduced by Yoon *et al.*[45] could be clearly ruled out due to our previous study on the influence of the oxidation potential of the photocatalysts on the reaction rate.[10]

The reason for the lower efficiency using the cooperative photocatalyst couple in comparison with the one catalyzed in the presence of sacrificial reagents might be caused by different factors. The multi-step electron transfer within the photocatalyst couple and further to the substrate might not be efficient due to the low concentration of the catalysts. Another important factor might be the electron transfer steps between the intermediates and the photogenerated hole. For this point, an additional study was conducted as described below.

The photo-induced electron transfer within the cooperative photocatalyst couple usually occurs based on the rather random contact between the two OSs in the liquid reaction medium. To create a non-random contact and thereby a more

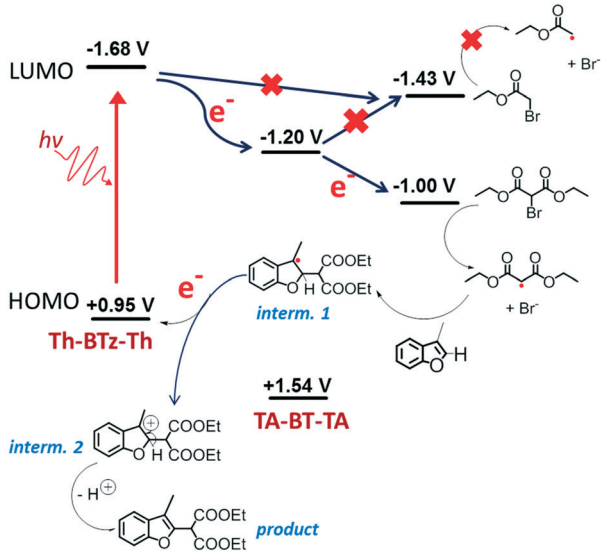

Fig. 3 Study of the electron transfer pathway using comparative substrates with different reduction potentials. Light source: white LED lamp (0.07 Wcm^{-2}, $\lambda > 420$ nm). Interm.: intermediate.

defined electron transfer process, we then connected Th-BTz-Th and TA-BT-TA *via* the C6 alkyl chain as a molecular bridge as a control photocatalyst. As displayed in Fig. 4c, a large molecule of Th-BTz-Th@TA-BT-TA containing both OSs in couple 2 was synthesized. Remarkably, the fluorescence intensity of Th-BTz-Th/TA-BT-TA strongly decreased after connection compared to their unconnected form as couple 2 (Fig. S8†). This result suggests a strong interaction between

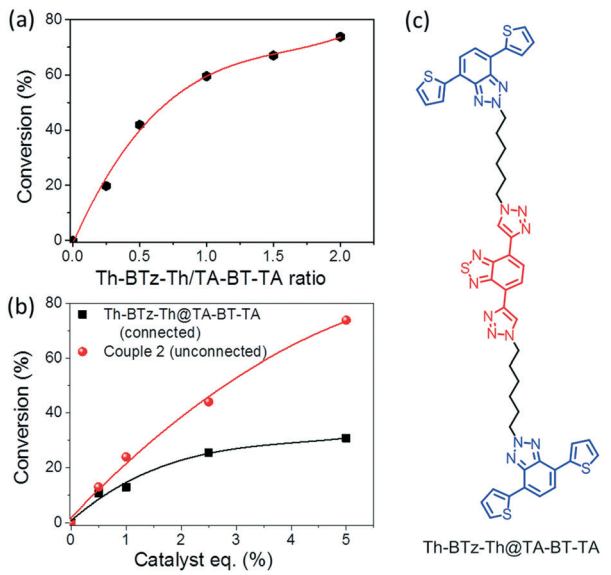

Fig. 4 Control experiments: (a) study of the impact of the OS ratio on the reaction conversion; (b) comparison between cooperative photocatalyst couple 2 with the C6-connected molecule Th-BTz-Th@TA-BT-TA; (c) structure of Th-BTz-Th@TA-BT-TA. Reaction conditions: 1 equiv. (0.38 mmol) 3-methylbenzofuran, 2 equiv. diethyl bromomalonate, 0.05 equiv. photocatalyst in 2.5 mL DMF, white LED (0.07 Wcm^{-2}, $\lambda > 420$ nm), 24 h, conversion determined by GC-MS.

the two OSs inside the large molecule. A study on the impact of Th-BTz-Th/TA-BT-TA in couple 2 on their photocatalytic efficiency showed that the highest reaction rate was achieved with a ratio of 2 : 1 of Th-BTz-Th/TA-BT-TA (Fig. 4a), which in fact corresponds to the connected molecule of Th-BTz-Th@TA-BT-TA. However, when comparing the catalytic efficiency between the connected catalyst Th-BTz-Th@TA-BT-TA and the unconnected couple 2 with the same ratio between both OSs, only a decreased conversion was observed for the connected catalyst (Fig. 4b). In spite of the better electron transfer occurring within connected system, the reduced catalytic efficiency could be likely caused by the steric hindrance within the large molecule or the competing charge recombination process,[46] which limits the contact between the substrate and the individual OSs in the large molecule and efficient electron transfer between the catalyst and substrate. To overcome this limitation, new molecular bridges other than the C6 alkyl chain could be needed.

Conclusions

In conclusion, we have taken the light-induced electron transfer cascade process in natural photosystems as a role model and developed a new sacrificial reagent-free photoredox pathway by employing molecular organic semiconductors as cooperative photocatalyst couples. The photocatalyst couples consists of two molecular organic semiconductors with complementary HOMO/LUMO band positions, leading to enhanced photo-induced intermolecular charge transfer between the organic photocatalysts within the couple. By the cooperative photocatalyst design, no extra electron-donating sacrificial reagents are needed and a new paradigm in the photoredox reaction without undesired side reactions under the oxidation of the sacrificial reagents can be established. We believe that the cooperative photocatalyst design ought not to be limited in chemical transformation reactions; it can also be applied in the field of photocatalytic water splitting or CO_2 reduction.

Experimental

Materials and methods

Chemicals were purchased from commercial sources and used as-received without further purification. 4,7-Dibromobenzo[*c*][1,2,5]thiadiazole (97%) was bought from Combi-Blocks. Sodium *tert*-butoxide (97%), *tert*-butanol (99.5%), sodium borohydride (96%), 1-bromobutane (99%), 2-(tributylstannyl)thiophene (97%), ethynyltrimethylsilane (98%), sodium ascorbate (98%), $Pd(PPh_3)Cl_2$ (98%), diethyl bromomalonate (92%), 3-methylbenzofuran (97%), 1-methylindole (97%) and 3-methylindole (98%) were bought from Sigma-Aldrich. Other commonly used solvents were bought from Fisher Scientific and VWR International. Glassware was dried under heating by a heating gun at 600 °C and cooled under vacuum prior to use if necessary. All photocatalyst reactions were conducted using common dry, inert atmosphere techniques *via* a Schlenk tube. The white LED (silent air

system white OL M-018) is a product of OSA Opto Light Gmbh with an intensity of 0.07 Wcm^{-2} from a distance of 5 cm. UV-vis absorption and emission spectra were recorded on a Perkin Elmer Lambda 100 spectrophotometer and a J&M TIDAS spectrofluorometer at ambient temperature, respectively. Cyclic voltammetry measurement was performed with an Autolab PGSTAT204 potentiostat/galvanostat of Metrohm (a three electrode cell system): a glassy carbon electrode as the working electrode, a $Hg/HgCl_2$ electrode as the reference electrode, a platinum wire as the counter electrode, and Bu_4NPF_6 (0.1 M Acetonitrile) as the supporting electrolyte with a scan rate of 100 mV s^{-1} in the range of −2 eV to 2.5 eV. ^1H and ^{13}C spectra were recorded on a Bruker Avance 300 spectrometer, and d-$CHCl_3$ was used as the solvent unless otherwise noted. GC-MS spectra were recorded on a SHIMADZU GCMS-QP2010 gas chromatograph mass spectrometer. Time-resolved photoluminescence (TRPL) on a nanosecond timescale was taken with a streak camera system (Hamamatsu C4742) in slow sweep mode. The excitation wavelength of 400 nm was provided using the frequency-doubled output of a commercial titanium:sapphire amplifier (Coherent LIBRA-HE, 3.5 mJ, 1 kHz, 100 fs).

Synthesis of the molecular organic semiconductor molecules

Synthesis of Th-BT-Th.[44] A 100 ml Schlenk tube equipped with a stirring bar and stopper was heated under vacuum then cooled three times before 4,7-dibromo-2,1,3-benzothiadiazole (1.76 g, 6.00 mmol), 2-(tributylstannyl)thiophene (4.76 ml, 15 mmol) and $Pd(PPh_3)_2Cl_2$ (201.60 mg, 5 mol%) were added. 30 ml anhydrous THF was added *via* a syringe and the reactor was degassed under vacuum and then back-filled with nitrogen three times. The mixture was heated at 90 °C overnight, then poured into 200 ml water and extracted with CH_2Cl_2 three times. The organic layer was washed with water twice and dried over anhydrous $MgSO_4$; the solvent was removed under vacuum. Purification with a short column then crystallization from methanol give a needle-like reddish solid (1.14 g, 63%). ^1H NMR (300 MHz, $CDCl_3$) δ: 8.04 (dd, J = 3.7, 1.2 Hz, 2H), 7.88 (s, 2H), 7.39 (dd, J = 5.1, 1.2 Hz, 2H), 7.15 (dd, J = 5.2, 3.7 Hz, 2H). ^{13}C NMR (300 MHz, $CDCl_3$) δ: 152.66, 139.36, 128.02, 127.52, 126.81, 126.02, 125.79.

Synthesis of Th-BTz-Th.

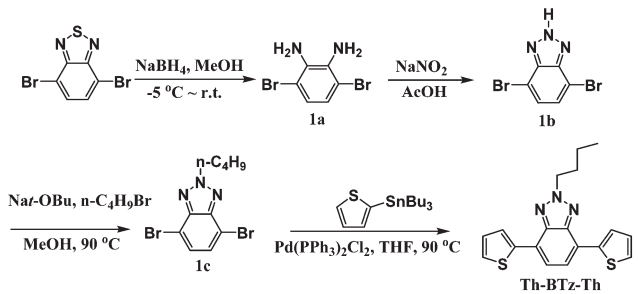

Synthesis of ***1a.*** The suspension of 4,7-dibromobenzo[*c*]-1,2,5-thiadiazole (2.94 g, 10 mmol) in 100 ml methanol was previously cooled to −5 °C in a water-ice bath. Then sodium borohydride (8 g, 21.7 mmol) was added portion-wise to the suspension. The mixture was warmed up to room temperature and stirred overnight. Then, 500 ml water was added, the mixture was extracted with CH_2Cl_2, the organic layer was washed with water twice and dried over anhydrous $MgSO_4$, and the solvent was removed under vacuum to give the final product as a pale yellow solid in 80% yield. The H-NMR data was consistent with the literature and the product used without further purification.[47]

Synthesis of ***1b.*** Dibromobenzene-1,2-diamine (2 g, 7.5 mmol) (**1a**) was added to a flask containing 15 ml glacial acetic acid. Sodium nitrite (1.03 g, 15 mmol) was dissolved in 10 ml water and added dropwise to the solution. The mixture was further reacted for another 3 hours before it was cooled with ice to 0 °C. The suspension was filtered and washed with water until the pH reached 7. The crude product was dried in an oven at 70 °C under vacuum overnight. The H-NMR data was consistent with the literature[1] and the product used without further purification.

Synthesis of ***1c.*** To a 100 ml Schlenk tube was added 4,7-dibromo-2*H*-benzo[*d*][1,2,3]triazole (2.4 g, 8.6 mmol) (**1b**) and Na*t*-OBu (1.24 g, 12.9 mmol), then 20 ml methanol and 1-bromobutyl (4.3 ml, 40 mmol) were added *via* a syringe. The mixture was degassed under vacuum slightly then back-filled with N_2 three times. After being stirred at 90 °C for 24 h, the mixture was poured into 200 ml water and extracted with CH_2Cl_2 three times. The organic layer was washed with water twice and dried over anhydrous $MgSO_4$; the solvent was removed under vacuum. Purification with a column using CH_2Cl_2/hexane = 1 : 1 as the eluent gave the final product as a white solid (1.28 g, 45%). ^1H NMR (300 MHz, $CDCl_3$) δ: 7.37 (s, 2H), 4.72 (t, J = 7.4 Hz, 2H), 2.06 (m, 2H), 1.41–1.29 (m, 2H), 0.91 (t, J = 7.4 Hz, 3H). ^{13}C NMR (300 MHz, $CDCl_3$) δ: 143.71, 129.51, 109.97, 57.22, 32.17, 19.82, 13.51.

Synthesis of Th-BTz-Th. A 100 ml Schlenk tube equipped with a stirring bar and stopper was heated under vacuum then cooled three times before 4,7-dibromo-2-(*n*-butyl)-2*H*-benzo[*d*]-[1,2,3]triazole (1 g, 3.00 mmol) (**1c**), 2-(tributylstannyl)thiophene (2.38 ml, 7.5 mmol) and $Pd(PPh_3)_2Cl_2$ (100.8 mg, 5 mol%) were added. 15 ml anhydrous THF was added *via* a syringe and the reactor was degassed under vacuum and then back-filled with nitrogen three times. The mixture was heated at 90 °C overnight, then poured into 200 ml water and extracted with CH_2Cl_2 three times. The organic layer was washed with water twice and dried over anhydrous $MgSO_4$; the solvent was removed under vacuum. Purification with a column using CH_2Cl_2/hexane = 1 : 1 as the eluent gave the final product as a light red solid (713 mg, 70%). ^1H NMR (300 MHz, $CDCl_3$) δ: 8.03 (dd, J = 3.7, 1.2 Hz, 2H), 7.56 (s, 2H), 7.31 (dd, J = 5.1, 1.2 Hz, 2H), 7.12 (dd, J = 5.1, 3.7 Hz, 2H), 4.76 (t, J = 7.4 Hz, 2H), 2.16–2.07 (m, 2H), 1.44–1.34 (m, 2H), 0.94 (t, J = 7.4 Hz, 3H). ^{13}C NMR (75 MHz, $CDCl_3$) δ: 142.10, 139.97, 128.12, 126.97, 125.55, 123.59, 122.78, 56.61, 32.08, 19.89, 13.57.

Synthesis of TA-BT-TA.

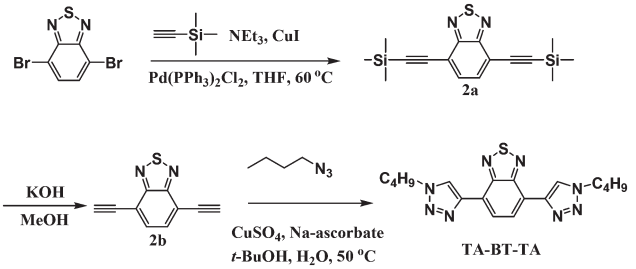

Synthesis of 2a. A 100 ml Schlenk tube equipped with a stirring bar and stopper was heated under vacuum then cooled three times before 4,7-dibromobenzothiadiazole (3 g, 10.2 mmol), $Pd(PPh_3)_2Cl_2$ (143.2 mg, 2%), CuI (77 mg, 4%) were added. 30 ml THF and 10 ml NEt_3 were added *via* a syringe. The mixture was cooled to freeze in liquid N_2, then trimethylsilyl acetylene (4 ml, 30.6 mmol) was added. The reactor was degassed *via* the freeze–pump–thaw method and the reaction mixture was stirred at 50 °C overnight. Then the mixture was poured into 100 ml water and extracted with CH_2Cl_2 three times. The organic layer was washed with water twice and dried over anhydrous $MgSO_4$; the solvent was removed under vacuum. Purification with a column using CH_2Cl_2/hexane = 1 : 1 as the eluent gave the final product as a light yellow solid (2.78 g, 83%). The H-NMR data was consistent with the literature reported.[48]

Synthesis of 2b. In a 100 ml two neck flask was added KOH methanol solution (1 mol L^{-1}, 50 ml) and 4,7-bis[2-(trimethylsilyl)ethynyl]benzothiadiazole (1 g, 3 mmol) (**2a**). The solution was stirred at room temperature for 2 h, and then it was poured into 300 ml water and extracted with CH_2Cl_2 three times. The organic layer was washed with water twice and dried over anhydrous $MgSO_4$; the solvent was removed under vacuum. Purification with a column using CH_2Cl_2/hexane = 1 : 1 as the eluent gave the final product as a light brown solid (420 mg, 876%). The H-NMR data was consistent with the literature reported.[48]

TA-BT-TA. 4,7-Diethynylbenzothiadiazole (400 mg, 2.17 mmol) (**2b**), 1-azidobutane (synthesis of 1-azidobutane: a mixture of 10 mmol 1-bromobutane and 20 mmol sodium azide in 100 ml DMSO was stirred overnight at RT, then the reaction mixture was poured into 500 ml water and extracted with CH_2Cl_2 then dried over anhydrous $MgSO_4$, the solvent was removed under vacuum, and the mixture was used as-synthesized without column purification. Caution: the excessive amount of sodium azide in the water phase must be slowly added to a solution of NaOCl before deposition). $CuSO_4$ (51.4 mg, 0.32 mmol), Na-ascorbate (87 mg, 0.44 mmol), 20 ml *t*-BuOH, 2 ml H_2O were added into a 100 ml two neck flask. The reactor was degassed under vacuum and then back-filled with nitrogen three times. The mixture was heated at 60 °C overnight, then poured into 200 ml water and extracted with CH_2Cl_2 three times. The organic layer was washed with water twice and dried over anhydrous $MgSO_4$; the solvent was removed under vacuum. Purification with a column using CH_2Cl_2/acetone = 10:1 as the eluent then re-crystallization from methanol gave the final product as a sheet-like yellow solid (747 mg, 90%). ^{1}H NMR (300 MHz, $CDCl_3$) δ: 8.67 (s, 2H), 8.61 (s, 2H), 4.44 (t, J = 7.4 Hz, 4H), 2.00–1.90 (m, 4H), 1.43–1.32 (m, 4H), 0.94 (t, J = 7.4 Hz, 6H). ^{13}C NMR (75 MHz, $CDCl_3$) δ: 152.29, 143.10, 126.08, 123.74, 122.66, 50.27,32.37, 19.79, 13.52.

Synthesis of the connected catalyst Th-BT-Th@TA-BT-TA.

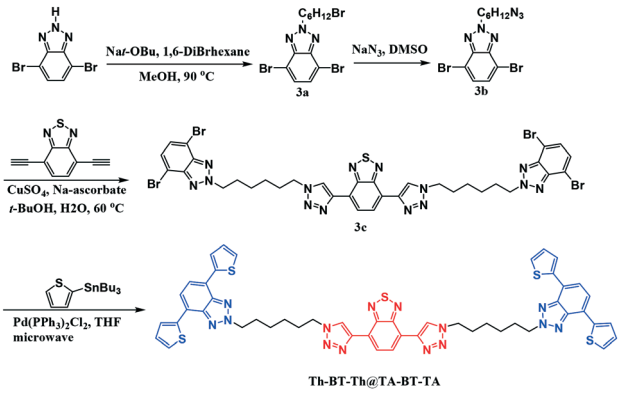

Synthesis of 3a. To a 100 ml Schlenk tube was added 4,7-dibromo-2*H*-benzo[*d*][1,2,3]triazole (3 g, 10.8 mmol) and Na*t*-OBu (1.56 g, 16.2 mmol), then 40 ml methanol and 1,6-dibromohexane (8.3 ml, 54 mmol) were added *via* a syringe. The mixture was degassed under vacuum slightly then back-filled with N_2 three times. After being stirred at 90 °C for 24 h, the mixture was poured into 200 ml water and extracted with CH_2Cl_2 three times. The organic layer was washed with water twice and dried over anhydrous $MgSO_4$; the solvent was removed under vacuum. Purification with a column using CH_2Cl_2/hexane = 1 : 1 as the eluent gave the final product as a white solid (1.82 g, 41%). ^{1}H NMR (300 MHz, $CDCl_3$) δ: 7.38 (s, 2H), 4.73 (t, J = 7.4 Hz, 2H), 3.33 (t, J = 7.4 Hz, 2H), 2.16–2.06 (m, 2H), 1.84–1.75 (multi, 2H), 1.50–1.39 (multi, 2H), 1.34–1.29 (multi, 2H). ^{13}C NMR (75 MHz, $CDCl_3$) δ: 143.76, 129.64, 110.00, 57.24, 33.58, 32.39, 29.99, 27.54, 25.70.

Synthesis of 3b. 4,7-Dibromo-2-(bromohexane)-benzo[*d*][1,2,3]triazole (1.8 g, 2.27 mmol) (**3a**) and sodium azide (295 mg, 4.54 mmol) were dissolved in 20 ml DMSO and stirred under room temperature overnight. Then the mixture was poured into 200 ml water and extracted with CH_2Cl_2 three times. The organic layer was washed with water twice and dried over anhydrous $MgSO_4$; the solvent was removed under vacuum. The product was used directly for the next step without any purification.

Synthesis of 3c. In a 100 ml two neck flask was added 4,7-diethynylbenzothiadiazole (184 mg, 1 mmol) (**3b**), 4,7-dibromo-2-(bromohexane)-benzo[*d*][1,2,3]triazole, $CuSO_4$ (24 mg, 0.15 mmol), Na-ascorbate (41 mg, 0.21 mmol), 10 ml *t*-BuOH, and 1 ml H_2O. The reactor was degassed under vacuum and then back-filled with nitrogen three times. The suspension was stirred under heating at 60 °C for two days, then

it was poured into 100 ml water and extracted with CH_2Cl_2 three times. The organic layer was washed with water twice and dried over anhydrous $MgSO_4$; the solvent was removed under vacuum. Purification with a column using CH_2Cl_2/acetone = 20 : 1 as the eluent gave the final product as a yellow solid (750 mg, 76%). ^{1}H NMR (300 MHz, $CDCl_3$) δ: 8.66 (s, 2H), 8.59 (s, 2H), 7.36 (s, 4H), 4.72 (t, J = 7.4 Hz, 4H), 4.42 (t, J = 7.4 Hz, 4H), 2.16–2.07 (m, 4H), 2.00–1.94 (m, 4H), 1.42–1.39 (m, 8H). ^{13}C NMR (75 MHz, $CDCl_3$) δ: 152.26, 143.74, 143.14, 129.65, 126.15, 123.82, 122.58, 109.98, 57.12, 50.30, 30.11, 29.86, 25.94.

Th-BT-Th@TA-BT-TA. In a capped vial, **3c** (750 mg, 0.76 mmol), 2-(tributylstannyl)thiophene (1.64 ml, 4.56 mmol) and $Pd(PPh_3)_2Cl_2$ (53 mg, 10 mol%) were added. 10 ml anhydrous THF was added *via* a syringe and the reactor was degassed *via* bubbling nitrogen for 5 min. The vial was put in a microwave reactor (120 °C, 0.8 T) for 1 h, then poured into 100 ml water and extracted with CH_2Cl_2 three times. The organic layer was washed with water twice and dried over anhydrous $MgSO_4$; the solvent was removed under vacuum. Purification with a column using CH_2Cl_2/acetone = 20 : 1 as the eluent gave the final product as a yellow-red solid (403 mg, 53%). ^{1}H NMR (300 MHz, $CDCl_3$) δ: 8.59 (s, 2H), 8.55 (s, 2H), 7.98 (dd, J = 3.7, 1.2 Hz, 4H), 7.52 (s, 4H), 7.29–7.27 (m, 4H), 7.08 (dd, J = 5.1, 3.7 Hz, 4H), 4.74 (t, J = 7.4 Hz, 4H), 4.39 (t, J = 7.4 Hz, 4H), 2.16–2.12 (m, 4H), 1.98–1.93 (m, 4H), 1.45–1.42 (m, 8H). ^{13}C NMR (75 MHz, $CDCl_3$) δ: 152.21, 143.15, 142.09, 139.84, 128.10, 126.92, 126.04, 125.63, 123.72, 123.55, 122.82, 122.59, 56.52, 50.30, 30.15, 29.70, 26.03, 25.97.

General procedure for the electron-donating sacrificial reagent-free and photocatalytic C–C bond formation reactions using cooperative photocatalyst systems

A 25 ml Schlenk tube equipped with a stirring bar and stopper was heated under vacuum then cooled for one hour and then back-filled with argon before the electron-rich heteroaromates (3-methyl benzofuran, *etc.*) (0.38 mmol, 1 equiv.), cooperative photocatalyst couple system (declared amount and ratio as described in Table 1), diethyl bromomalonate (0.76 mmol, 2.0 equiv.), 2.5 ml DMF were added. The reactor was degassed *via* the freeze–pump–thaw method and irradiated under a white LED lamp (0.07 W cm^{-2}) in a water bath (see the photograph in the ESI†) for 24 h. The conversion was determined *via* GC-MS and the pure product was obtained *via* chromatography.

Comparison control experiment for the C–C bond formation reactions between 3-methylbenzofuran and ethyl bromoacetate using Th-BTz-Th as a catalyst and 4-methoxyltriphenylamine as an electron-donating sacrificial reagent

A 25 ml Schlenk tube equipped with a stirring bar and stopper was heated under vacuum then cooled for one hour and then back-filled with argon before 3-mehtylbenzofuran (0.38 mmol, 1 equiv.), 4-methoxyltriphenylamine (0.76 mmol, 2 equiv.), ethyl bromomalonate (0.76 mmol, 2.0 equiv.), Th-BTz-Th (1 mol%), and 2.5 ml DMF were added. The reactor was degassed *via* the freeze–pump–thaw method and irradiated under a white LED. The reaction time was determined by GC-MS when the signal of the starting material totally disappeared. After the reaction was completed, the mixture was poured into 20 ml water and extracted with CH_2Cl_2, the organic layer was dried over anhydrous $MgSO_4$, and the solvent was removed under vacuum. The crude product was purified on silica gel using the indicated solvent system to obtain the desired product. ^{1}H NMR (300 MHz, $CDCl_3$) δ: 7.40–7.32 (m, 2H), 7.20–7.11 (m, 2H), 4.11 (q, J = 7.4 Hz, 2H), 3.69 (s, 3H), 2.13 (s, 3H), 1.19 (t, J = 7.4 Hz, 3H). ^{13}C NMR (75 MHz, $CDCl_3$) δ: 169.14, 154.15, 146.12, 129.91, 123.92, 122.23, 119.13, 112.81, 110.95, 61.35, 32.84, 14.19, 7.97. Molecular weight $C_{13}H_{14}O_3$: calculated 218.09, found 218.10.

Conflicts of interest

The authors declare no conflict of interest.

Acknowledgements

The authors thank the Max Planck Society for financial support. L. W. thanks the China Scholarship Council (CSC) for scholarship. The work of I. R. is part of the research program of the Dutch Polymer Institute (project #763). Open Access funding provided by the Max Planck Society.

Notes and references

1 C. K. Prier, D. A. Rankic and D. W. C. MacMillan, *Chem. Rev.*, 2013, **113**, 5322–5363.
2 T. Kawai and T. Sakata, *Nature*, 1980, **286**, 474.
3 X. Wang, K. Maeda, A. Thomas, K. Takanabe, G. Xin, J. M. Carlsson, K. Domen and M. Antonietti, *Nat. Mater.*, 2009, **8**, 76–80.
4 D. P. Hari, P. Schroll and B. König, *J. Am. Chem. Soc.*, 2012, **134**, 2958.
5 M. Baar and S. Blechert, *Chem. – Eur. J.*, 2015, **21**, 526–530.
6 M. Woźnica, N. Chaoui, S. Taabache and S. Blechert, *Chem. – Eur. J.*, 2014, **20**, 14624–14628.
7 Q. Liu, H. Yi, J. Liu, Y. Yang, X. Zhang, Z. Zeng and A. Lei, *Chem. – Eur. J.*, 2013, **19**, 5120–5126.
8 I. Ghosh, T. Ghosh, J. I. Bardagi and B. König, *Science*, 2014, **346**, 725–728.
9 L. Furst, B. S. Matsuura, J. M. R. Narayanam, J. W. Tucker and C. R. J. Stephenson, *Org. Lett.*, 2010, **12**, 3104–3107.
10 L. Wang, W. Huang, R. Li, D. Gehrig, P. W. Blom, K. Landfester and K. A. Zhang, *Angew. Chem., Int. Ed.*, 2016, **55**, 9783–9787.
11 J. Schneider and D. W. Bahnemann, *J. Phys. Chem. Lett.*, 2013, **4**, 3479–3483.
12 Y. Tachibana, L. Vayssieres and J. R. Durrant, *Nat. Photonics*, 2012, **6**, 511.

13 M. Wang, K. Han, S. Zhang and L. Sun, *Coord. Chem. Rev.*, 2015, **287**, 1–14.
14 M. Yamamoto, L. Wang, F. Li, T. Fukushima, K. Tanaka, L. Sun and H. Imahori, *Chem. Sci.*, 2016, **7**, 1430–1439.
15 M. F. Kuehnel, K. L. Orchard, K. E. Dalle and E. Reisner, *J. Am. Chem. Soc.*, 2017, **139**, 7217–7223.
16 N. A. Romero and D. A. Nicewicz, *Chem. Rev.*, 2016, **116**, 10075–10166.
17 D. A. Nicewicz and T. M. Nguyen, *ACS Catal.*, 2014, **4**, 355–360.
18 D. J. Wilger, N. J. Gesmundo and D. A. Nicewicz, *Chem. Sci.*, 2013, **4**, 3160.
19 S. Fukuzumi and K. Ohkubo, *Chem. Sci.*, 2013, **4**, 561–574.
20 M. Neumann, S. Fueldner, B. Koenig and K. Zeitler, *Angew. Chem., Int. Ed.*, 2011, **50**, 951.
21 K. Zhang, D. Kopetzki, P. H. Seeberger, M. Antonietti and F. Vilela, *Angew. Chem., Int. Ed.*, 2013, **52**, 1432–1436.
22 N. Kang, J. H. Park, K. C. Ko, J. Chun, E. Kim, H. W. Shin, S. M. Lee, H. J. Kim, T. K. Ahn, J. Y. Lee and S. U. Son, *Angew. Chem., Int. Ed.*, 2013, **52**, 6228–6232.
23 K. Zhang, Z. Vobecka, K. Tauer, M. Antonietti and F. Vilela, *Chem. Commun.*, 2013, **49**, 11158–11160.
24 J. Luo, X. Zhang and J. Zhang, *ACS Catal.*, 2015, **5**, 2250–2254.
25 Z. J. Wang, S. Ghasimi, K. Landfester and K. A. Zhang, *Adv. Mater.*, 2015, **27**, 6265–6270.
26 R. S. Sprick, J.-X. Jiang, B. Bonillo, S. Ren, T. Ratvijitvech, P. Guiglion, M. A. Zwijnenburg, D. J. Adams and A. I. Cooper, *J. Am. Chem. Soc.*, 2015, **137**, 3265–3270.
27 S. Ghasimi, S. Prescher, Z. J. Wang, K. Landfester, J. Yuan and K. A. I. Zhang, *Angew. Chem., Int. Ed.*, 2015, **54**, 14549–14553.
28 C. Yang, B. C. Ma, L. Zhang, S. Lin, S. Ghasimi, K. Landfester, K. A. I. Zhang and X. Wang, *Angew. Chem., Int. Ed.*, 2016, **55**, 9202–9206.
29 R. S. Sprick, B. Bonillo, R. Clowes, P. Guiglion, N. J. Brownbill, B. J. Slater, F. Blanc, M. A. Zwijnenburg, D. J. Adams and A. I. Cooper, *Angew. Chem., Int. Ed.*, 2016, **55**, 1792–1796.
30 G. Zhang, Z.-A. Lan and X. Wang, *Angew. Chem., Int. Ed.*, 2016, **55**, 15712–15727.
31 S. Ventre, F. R. Petronijevic and D. W. C. MacMillan, *J. Am. Chem. Soc.*, 2015, **137**, 5654–5657.
32 J. D. Cuthbertson and D. W. C. MacMillan, *Nature*, 2015, **519**, 74–77.
33 E. L. Tyson, M. S. Ament and T. P. Yoon, *J. Org. Chem.*, 2013, **78**, 2046–2050.
34 L. R. Espelt, I. S. McPherson, E. M. Wiensch and T. P. Yoon, *J. Am. Chem. Soc.*, 2015, **137**, 2452–2455.
35 J. D. Nguyen, E. M. D'Amato, J. M. R. Narayanam and C. R. J. Stephenson, *Nat. Chem.*, 2012, **4**, 854–859.
36 C. J. Yao, Q. Sun, N. Rastogi and B. Konig, *ACS Catal.*, 2015, **5**, 2935–2938.
37 E. Brachet, T. Ghosh, I. Ghosh and B. Konig, *Chem. Sci.*, 2015, **6**, 987–992.
38 R. Brimioulle, D. Lenhart, M. M. Maturi and T. Bach, *Angew. Chem., Int. Ed.*, 2015, **54**, 3872–3890.
39 J. W. Tucker, J. M. R. Narayanam, S. W. Krabbe and C. R. J. Stephenson, *Org. Lett.*, 2010, **12**, 368–371.
40 J. W. Tucker and C. R. J. Stephenson, *J. Org. Chem.*, 2012, **77**, 1617–1622.
41 J. Snellenburg, S. Laptenok, R. Seger, K. Mullen and I. Van Stokkum, *J. Stat. Softw.*, 2012, **49**, 1–22.
42 M. C. Scharber, D. Mühlbacher, M. Koppe, P. Denk, C. Waldauf, A. J. Heeger and C. J. Brabec, *Adv. Mater.*, 2006, **18**, 789–794.
43 J. Halls, J. Cornil, D. Dos Santos, R. Silbey, D.-H. Hwang, A. Holmes, J. Brédas and R. Friend, *Phys. Rev. B: Condens. Matter Mater. Phys.*, 1999, **60**, 5721.
44 L. Wang, W. Huang, R. Li, D. Gehrig, P. W. Blom, K. Landfester and K. A. Zhang, *Angew. Chem., Int. Ed.*, 2016, **55**, 9783–9787.
45 M. A. Cismesia and T. P. Yoon, *Chem. Sci.*, 2015, **6**, 5426–5434.
46 S. Ando, C. Ramanan, A. Facchetti, M. R. Wasielewski and T. J. Marks, *J. Mater. Chem.*, 2011, **21**, 19049–19057.
47 J.-H. Kim, H. U. Kim, C. E. Song, I.-N. Kang, J.-K. Lee, W. S. Shin and D.-H. Hwang, *Sol. Energy Mater. Sol. Cells*, 2013, **108**, 113–125.
48 Y. Lei, H. Li, W. Gao, M. Liu, J. Chen, J. Ding, X. Huang and H. Wu, *J. Mater. Chem. C*, 2014, **2**, 7402–7410.